Poleward Transport of African Dust to the Iberian Peninsula Organized by Multiscale Terrain-Induced Circulations: Observations and High-Resolution WRF-Chem Simulation Analyses

Saroj Dhital, Michael L. Kaplan, Jose Antonio Garcia Orza, and Stephanie Fiedler

Division of Atmospheric Sciences, Desert Research Institute, Reno, NV, USA, Department of Applied Aviation Sciences, Embry-Riddle Aeronautical University, Prescott, AZ, USA, SCOLAb, Dept. of Physics, Universidad Miguel Hernandez, Elche, Spain, Institute of Geophysics and Meteorology, University of Colonge, Köln, Germany

PRESENTED AT:

AGU FALL MEETING
Online Everywhere | 1–17 December 2020

INTRODUCTION, MOTIVATION, AND RESEARCH OBJECTIVES

Introduction and Motivation

- An extreme African dust outbreak occurred during 20-21 February 2016 over the Iberian Peninsula (IP), the southwest corner of Europe.
- Two distinct dust plumes reached the IP in succession [1].
- Nearly 90% of the air quality stations in Spain exceeded the European Union's PM_{10} daily limit of 50 $\mu g.m^{-3}$ [2].
- We analyze the mesoscale meteorological processes responsible in organizing this dust outbreak to Europe.

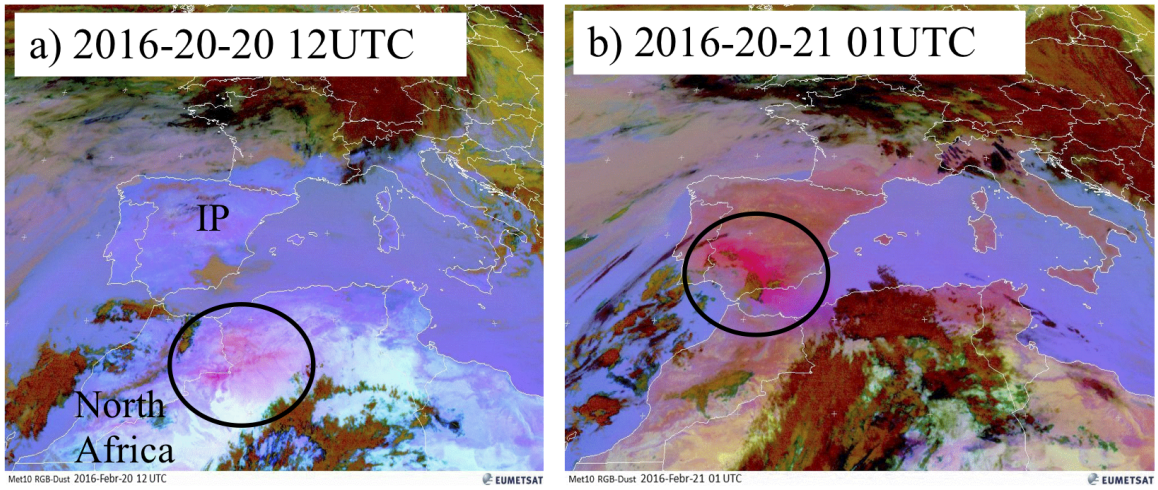

Figure 1: False-color dust RGB from the SEVIRI instrument for (a) 12 UTC 20 and (b) 01 UTC 21 February 2016, where magenta color indicates dust. The black circles show the poleward propagating dust plume.

Research Objectives

- Understand the terrain-induced mesoscale circulations instrumental for dust ablation and subsequent poleward transport to the IP.
- The possible use of the WRF-Chem model in operational dust forecasting.

DATASETS, NUMERICAL SIMULATION, AND MODEL EVALUATION

Datasets and Numerical Simulation

- False-color dust RGB from the SEVIRI instrument.
- Meteorological Terminal Aviation Routine Weather Report.
- ECMWF ERA-Interim reanalysis products [3].
- Aerosol optical depth from the MODIS satellite.
- WRF-Chem model utilizing the GOCART dust scheme [4].

WRF-Chem model setup

No. of domains: 3

Total simulation hours: 52 hours

Horizontal resolutions: 18, 6, and 2 km

Model vertical structure: 40 levels

Model initialization: Era-Interim dataset

Model physical parameterization: Follows a similar study over North Africa [5].

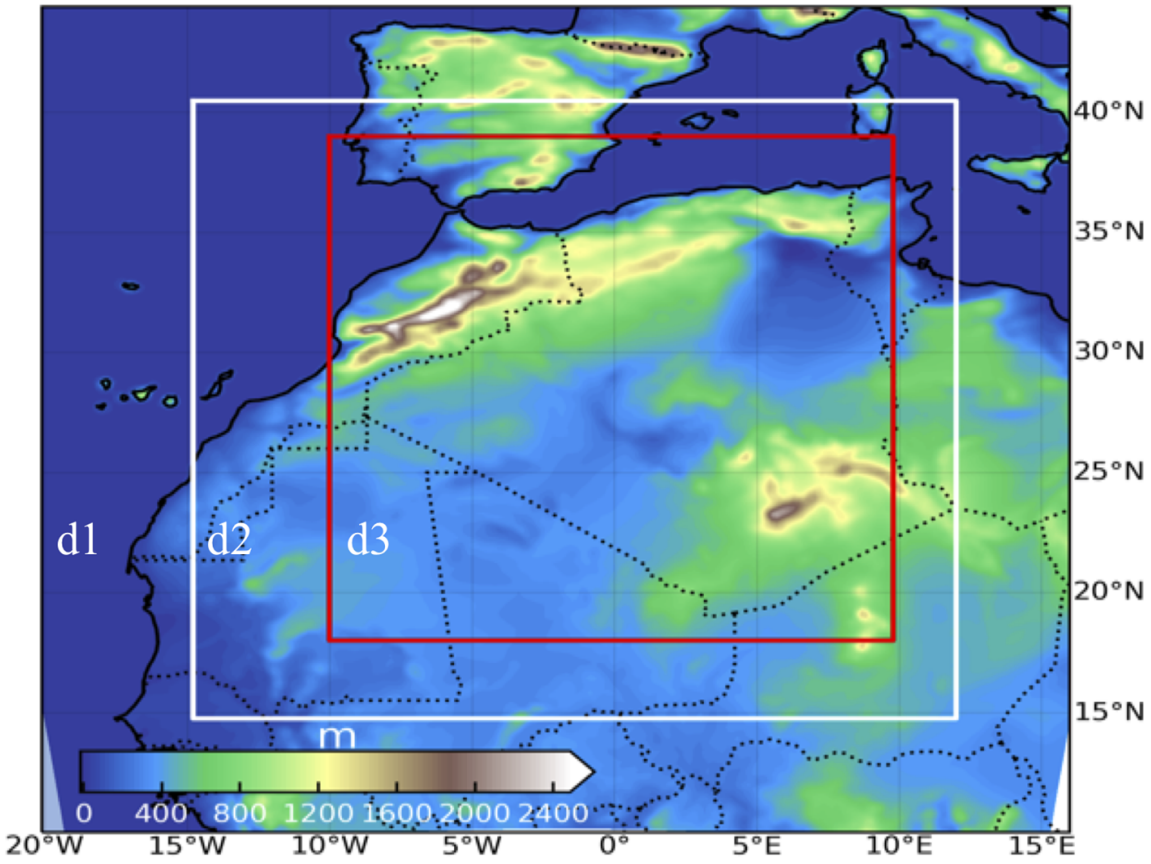

Figure 2: WRF-Chem simulation domain.

Model evaluation

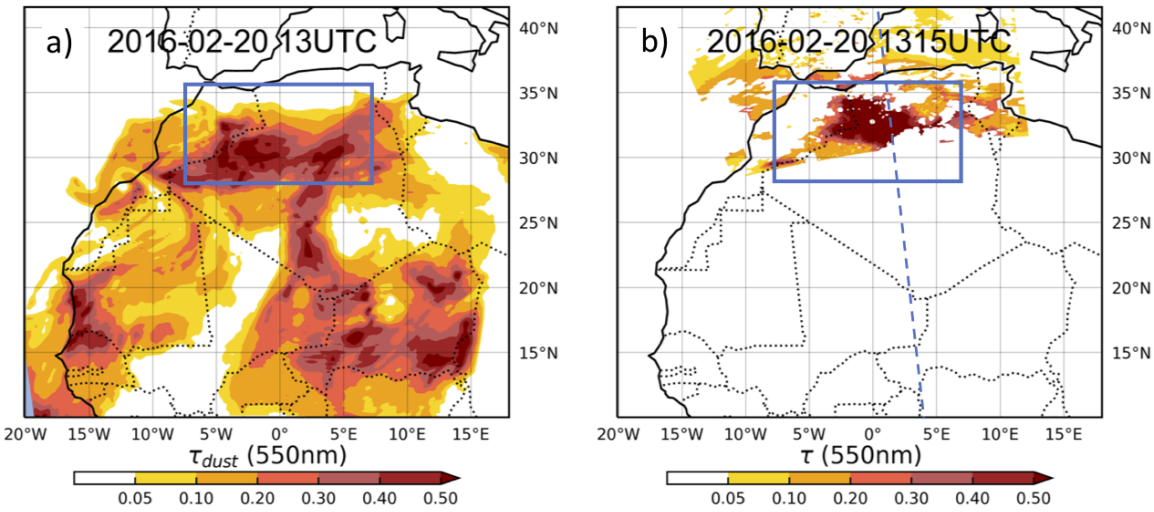

Figure 3: Aerosol optical depth (τ). Shown are the (a) WRF-Chem simulated (18 km) dust τ at 13 UTC 20 February 2016 and the (b) Dark Target Deep Blue combined τ at 550 nm from the MODIS aboard Aqua at 1315 UTC 20 February 2016. The dashed blue line represents the MODIS Aqua overpass. Blue boxes indicate the poleward propagating dust plumes over the Saharan Atlas Mountains (SAM).

RESULTS

Barrier Jet (BJ)

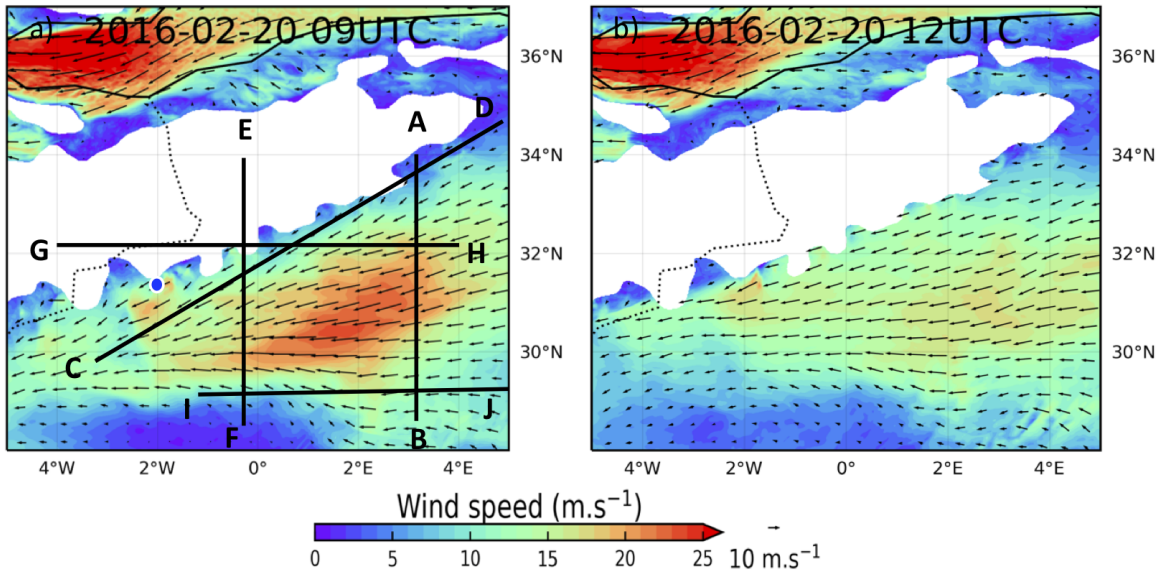

Figure 4: WRF-Chem simulated (2 km) 925 hPa horizontal wind vector and speed (fill in m.s-1) at (a) 09 UTC and (b) 12 UTC on 20 February 2016. The solid black lines mark cross-sections used in later analyses: A-B (28°N, 3°E to 34°N, 3°E), C-D (30°N, 3.5°W to 34.5°N, 5°E), E-F (28°N, 0.28°W to 34°N, 0.28°W), G-H (32.38°N, 4°W to 32.38°N, 4°E), I-J (29°N, 1°W to 29°N, 7°E). The white area represents elevation above the pressure levels.

Flow blocking for BJ

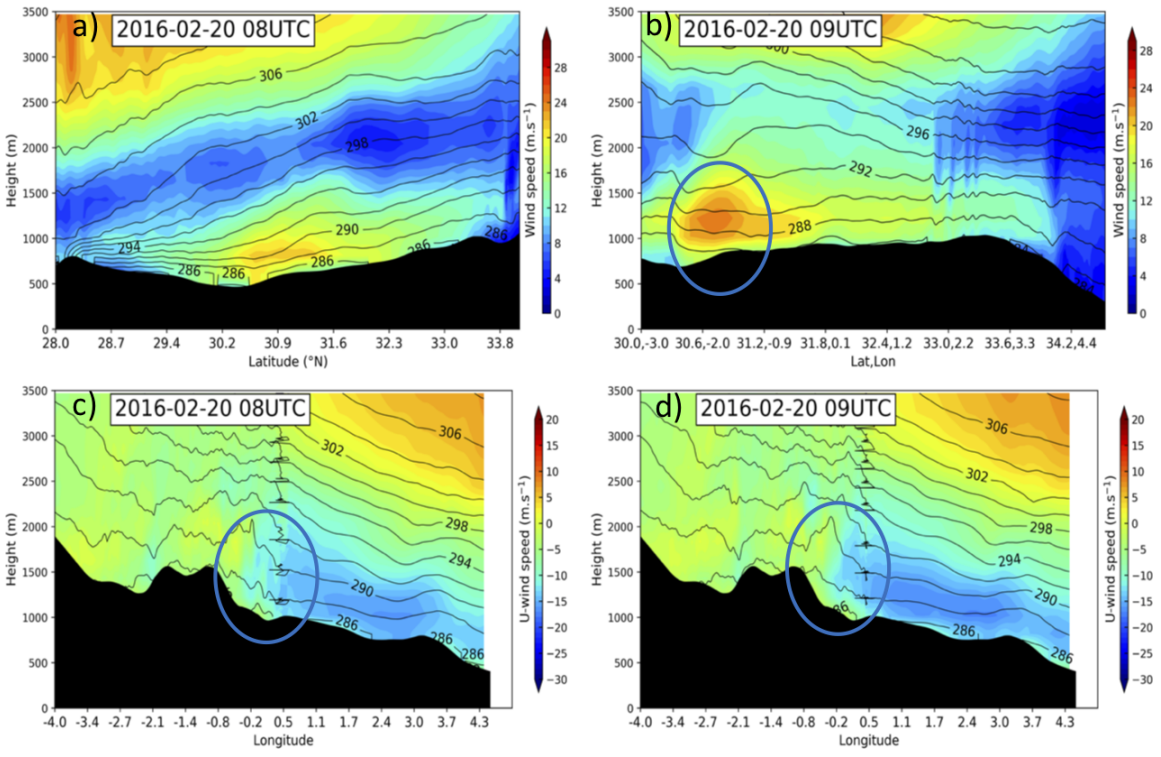

Figure 5: Horizontal winds and potential temperature transects for the first dust storm. Shown are simulation (2 km) results for the vertical cross-sections of potential temperature (lines in K) and wind speed (fill in m.s-1) at (a) 08 UTC along the line A-B and (b) 09 UTC along the line C-D on 20 February 2016. Vertical cross-section of potential temperature and u-wind speed along the line G-H at (c) 08 UTC and (d) at 09 UTC on 20 February 2016. Locations of the transects are marked in Fig. 4a. The circle in Figure b marks the BJ, in c and d the flow blocking.

RESULTS

Hydraulic Jumps

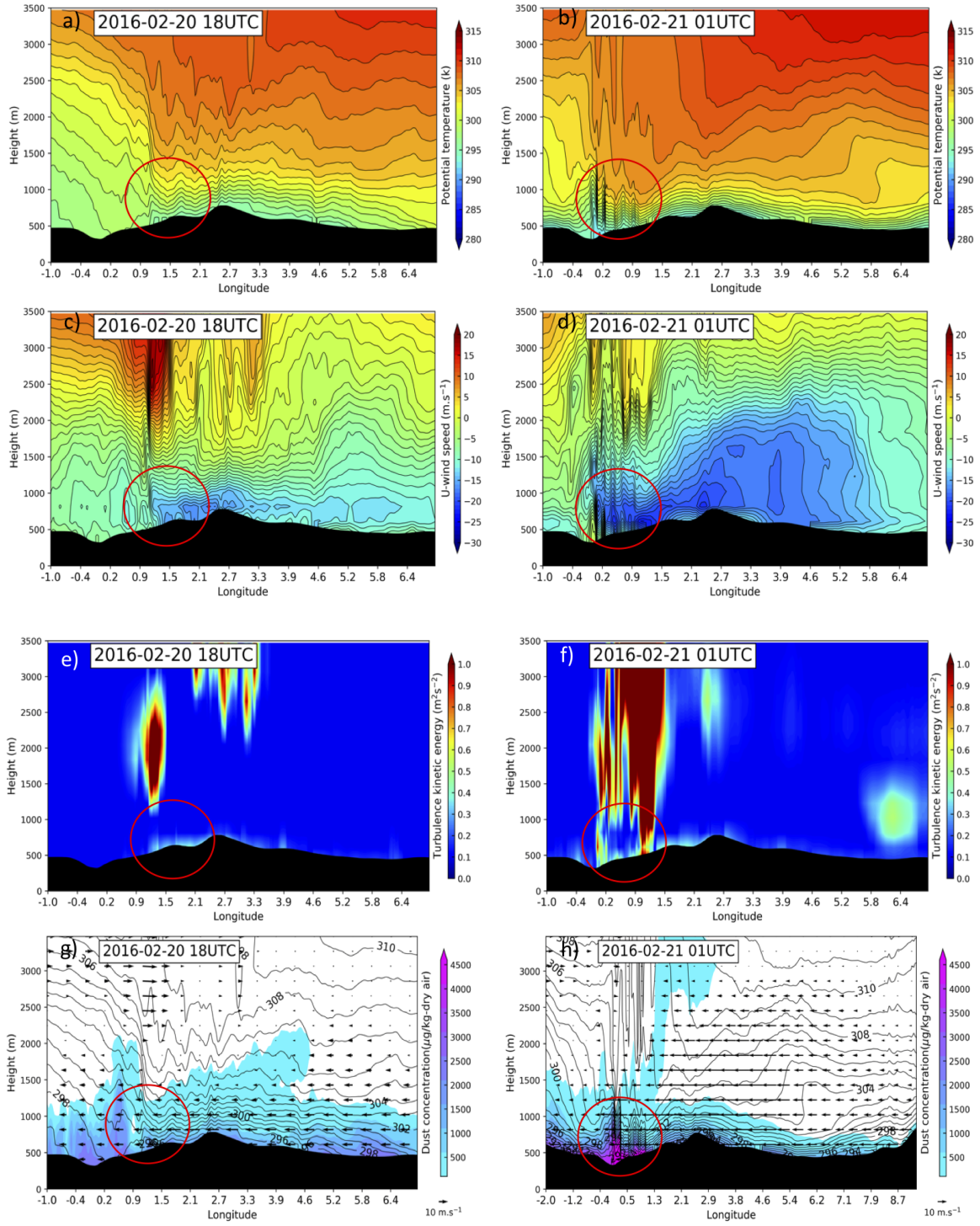

Figure 6: East-West transect along the line I-G for the second dust storm. Shown are WRF-Chem results (2 km) for the vertical cross-sections at 18 UTC on 20 February (left column) and 01 UTC on 21 February (right column) for (a, b) potential temperature, (c, d) u-wind component, (e, f) planetary boundary layer (PBL) turbulence kinetic energy (TKE, fill in m2.s-2), and (g, h) potential temperature (line in K), wind vector (u, w) and dust concentration. The circle marks the region of the hydraulic jump, increasing wind, and dust concentration.

RESULTS

Multiple dust plumes and poleward transport of dust

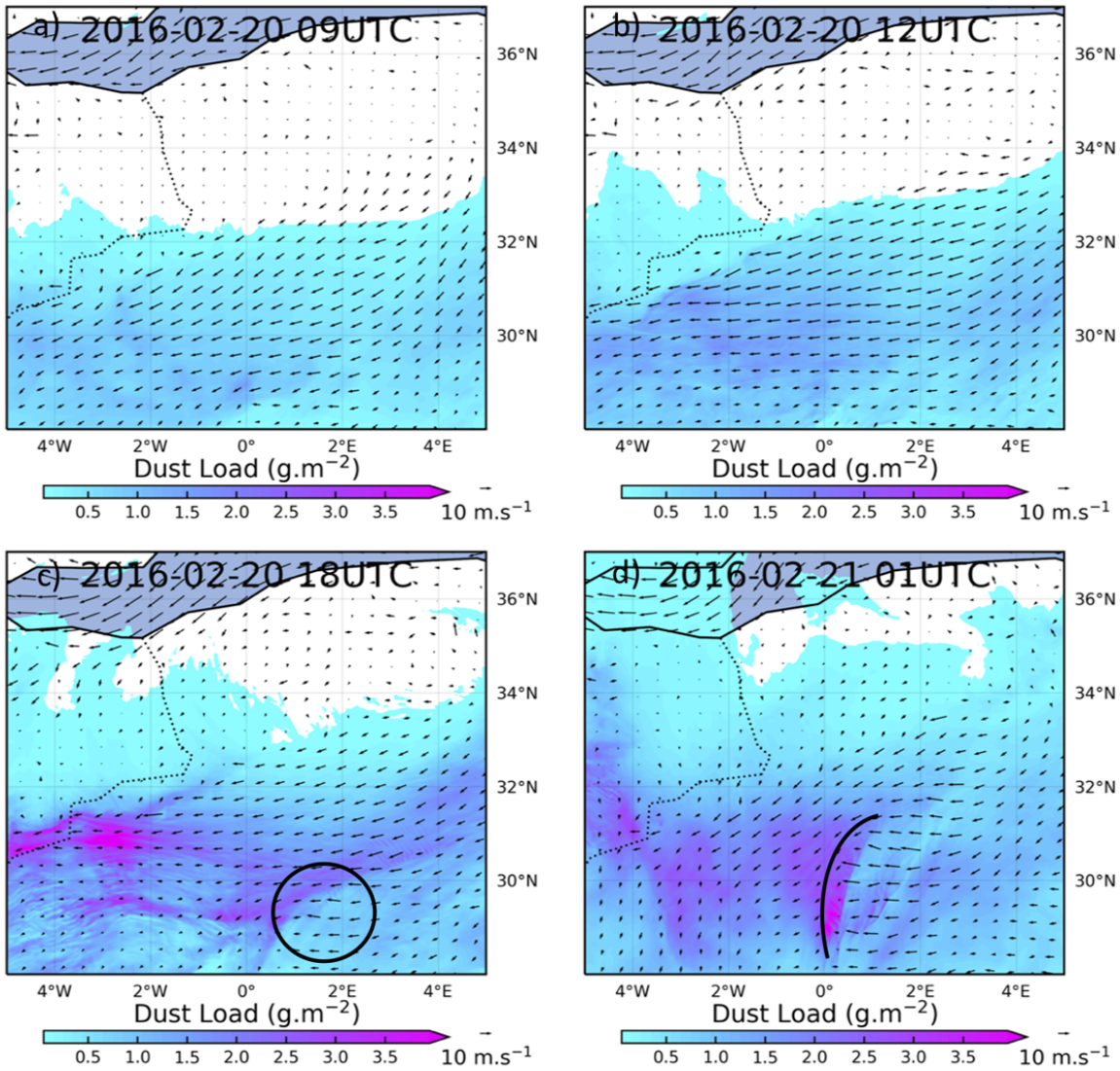

Figure 7: WRF-chem simulated (2 km) 10m wind vector (m.s-1) and dust load (fill in g.m-2) at (a) 09 UTC, (b) 12 UTC, (c) 20 UTC on 20 and (d) 01 UTC on 21 February 2016. The black circle in Figure c marks the region of increasing 10m wind. The black line in Figure d marks the second dust front.

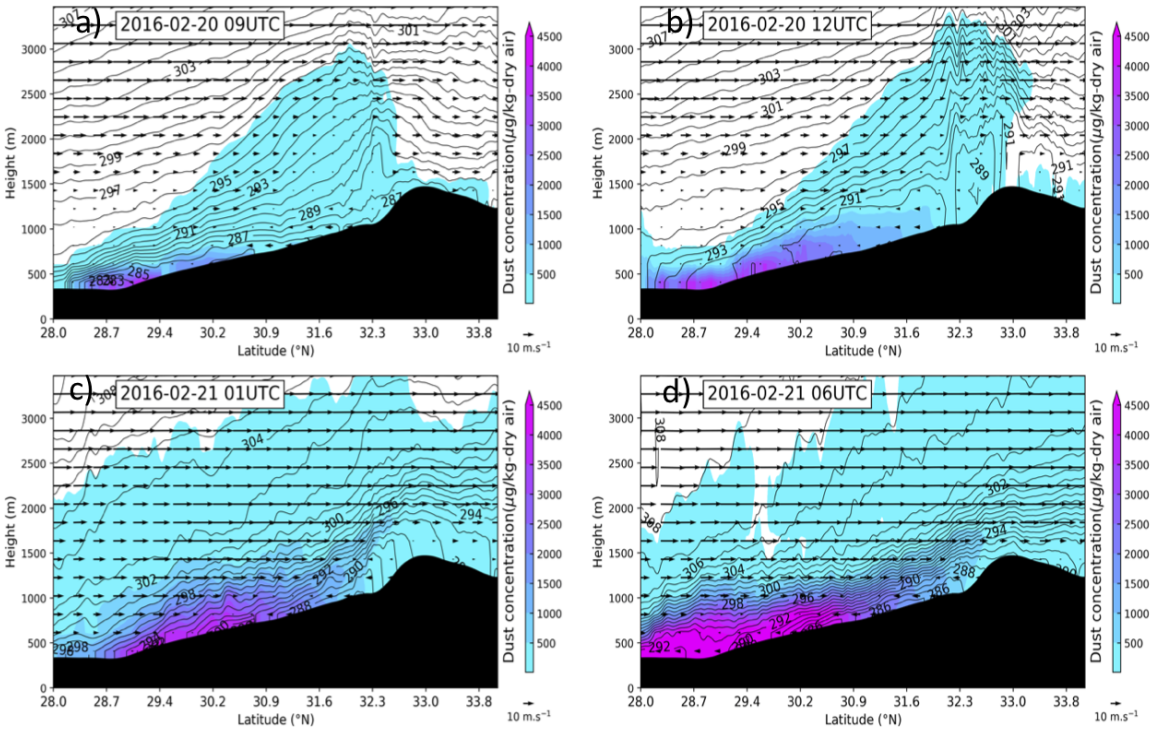

Figure 8: North-South transect along the line E-F. WRF-Chem results (2 km) for the vertical cross-section of potential temperature (K), wind vector (v and w, m.s-1), and dust concentration at the line E-F at (a) 09 UTC and (b) 12 UTC on 20 February 2016, and (c) 01 UTC and (d) 06 UTC on 21 February 2016.

SUMMARY AND CONCLUSIONS

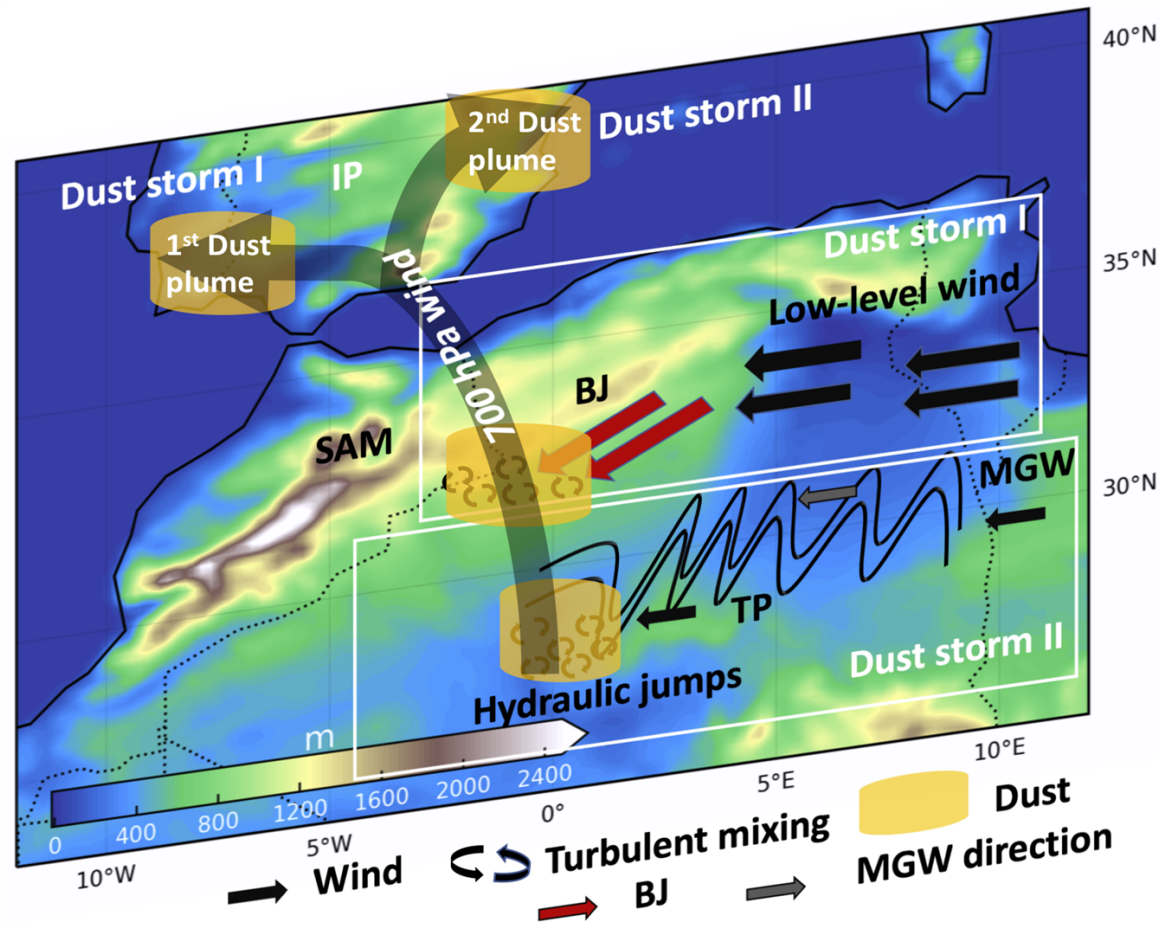

Figure 9: Schematic depiction of the time and location of the BJ and hydraulic jumps associated with MGW and subsequent transport of dust to the IP. Red arrow represents the BJ and gray arrow represents the MGW propagation direction.

- This dust outbreak comprised of two distinct phases of dust emission.
- In phase I, BJ formed on the southeastern foothills of the SAM and emitted a massive amount of dust on 20 February 2016 and resulted in the first dust plume.
- In phase II, the mesoscale gravity wave (MGW) affected the west of the Tinrhert Plateau during the morning of 20 February 2016.

- The MGW triggered multiple hydraulic jumps on the western flank of the Tademaït Plateau (TP).

- The strong downslope wind and TKE accompanying the hydraulic jumps enhanced the dust emission on the lee side of the TP and resulted in the second dust plume on 21 February 2016.

- The lifted dust extended over 2-3 km in altitude due to increasing convective turbulence in the growing daytime PBL.

- The predominant southerly/southeasterly mid-tropospheric flow subsequently advected the dust plume poleward to the IP.

- Our results underline the importance of resolving terrain-induced mesoscale processes to understand dust storm dynamics, which are difficult to represent in coarse-resolution numerical models.

ABSTRACT

This study presents the meso-β/γ scale dynamical features involved in an extreme African dust outbreak, which occurred during 20-21 February 2016 over the Iberian Peninsula (IP), the southwest corner of Europe. During this episode, nearly 90% of the air quality stations in Spain exceeded the European Union's PM_{10} daily limit. We used observations and performed nested-grid 2km simulations with the Weather Research and Forecasting model using coupled Chemistry (WRF-Chem) to understand the development of this dust outbreak. The surface observations and the false-color RGB dust product from the Spinning Enhanced Visible and Infrared Imager (SEVIRI) revealed that the dust storm was initiated on the southeastern flank of the Saharan Atlas Mountains at two distinct phases of dust emissions. The first dust plume crossed the Saharan Atlas during midday on the 20th, the second one followed in the afternoon of the 21st. The first dust plume was advected towards the Western IP, while the second one towards the Eastern IP. The WRF-Chem simulation results indicated that the phase I dust emission was associated with strong barrier jet (BJ) formation on the southeastern foothills of the Saharan Atlas Mountains. The BJ strengthened just after sunrise on the 20th and emitted a massive amount of dust resulting in the first strong dust storm. In phase II, a long-lived westward propagating mesoscale gravity wave (MGW) was triggered near the northeastern edge of the Tinrhert Plateau in eastern Algeria. When this westward propagating long-lived MGW crossed the Tademaït Plateau, multiple hydraulic jumps were formed on its lee side. The strong winds accompanying these multiple hydraulic jumps emitted and mixed dust aerosols upwards which enabled the second strong dust plume to reach the IP. The lifted dust extended over 2-3 km in altitude in the growing daytime planetary boundary layer (PBL) and was advected poleward by the southerly/southeasterly wind at 700hPa. Our results underline the importance of resolving meso-scale processes to understand dust storm dynamics in detail, which are difficult to represent in coarse-resolution (aerosol-) climate models.

REFERENCES

1. Orza, J. A. G., Dhital, S., Fiedler, S., & Kaplan, M. L. (2020). Large scale upper-level precursors for dust storm formation over North Africa and poleward transport to the Iberian Peninsula. Part I: An observational analysis. *Atmospheric Environment, 237*, 117688. https://doi.org/10.1016/j.atmosenv.2020.117688 (https://doi.org/10.1016/j.atmosenv.2020.117688).

2. Titos, G., Ealo, M., Pandolfi, M., Pérez, N., Sola, Y., Sicard, M., et al., (2017). Spatiotemporal evolution of a severe winter dust event in the western Mediterranean: aerosol optical and physical properties. *Journal of Geophysical Research: Atmospheres 122*, 4052–4069. https://doi.org/10.1002/2016JD026252 (https://doi.org/10.1002/2016JD026252)

3. Dee, D. P., Uppala, S. M., Simmons, A. J., Berrisford, P., Poli, P., Kobayashi, S., et al. (2011). The ERA-Interim reanalysis: Configuration and performance of the data assimilation system. *Quarterly Journal of the Royal Meteorological Society, 137*(656), 553–597. https://doi.org/10.1002/qj.828 (https://doi.org/10.1002/qj.828).

4. Ginoux, P., Chin, M., Tegen, I., Prospero, J. M., Holben, B., Dubovik, O., and Lin, S. J.: Sources and distributions of dust aerosols simulated with the GOCART model. *Journal of Geophysical Research: Atmospheres, 106*, 20255–20273.https://doi.org/10.1029/2000JD000053. (https://doi.org/10.1029/2000JD000053)

5. Dhital, S., Kaplan, M. L., Orza, J. A. G., & Fiedler, S. (2020). Atmospheric dynamics of a Saharan dust outbreak over Mindelo, Cape Verde Islands, preceded by Rossby wave breaking: Multiscale observational analyses and simulations. *Journal of Geophysical Research: Atmospheres, 125*, e2020JD032975. https://doi.org/10.1029/2020JD032975 (https://doi.org/10.1029/2020JD032975).